

Supporting information for

Solid State p-Type Dye Sensitized NiO-dye-TiO₂ Core-Shell Solar Cells

Lei Tian^a, Jens Föhlinger^a, Zhibin Zhang^b, Palas Baran Pati^a, Junzhong Lin^c, Tomas Kubart^b, Yong Hua^d, Junliang Sun^c, Lars Kloo^d, Gerrit Boschloo¹, Leif Hammarström^a, Haining Tian^{a,*}

a Department of Chemistry-Ångström Lab., Uppsala University, Sweden

b Department of Engineering Sciences, Uppsala University, Sweden

c Department of Materials and Environmental Chemistry, Stockholm University, Sweden

Preparation of electrodes

NiO-PB6-TiO₂ and NiO-TiO₂ electrodes were fabricated with the same method described in our previous study¹. The electrodes NiO-PB6-Al₂O₃-TiO₂, NiO-Al₂O₃-TiO₂ and NiO-PB6-Al₂O₃ with extra inner Al₂O₃ layers deposited by Atomic Layer Deposition before TiO₂ coating are prepared as following..

Atomic layer deposition (ALD) of Al₂O₃

The Al₂O₃ was deposited by using trimethyl aluminium (TMA) and H₂O under 70 °C, and each precursor was pulsed for 0.1 s, followed by 8 s and 15 s nitrogen purge to remove the unreacted TMA and H₂O, respectively. The Growth Per Cycle (GPC) was measured by ellipsometry on film deposited on a polished silicon wafer, and an averaged GPC value of 0.8 Å/cycle was obtained. The thickness of Al₂O₃ mentioned in this paper was calculated by the different deposition cycles on basis of 0.8 Å /cycle.

The TEM characterization could be the best way to monitor the thickness of the Al₂O₃ layer in such microporous film. However, it was hard to be observed directly due to the ultra-thin Al₂O₃ in the **NiO-PB6-Al₂O₃-TiO₂** electrode, like ca. 1 nm as evaluated in this paper. The amplified TEM image was shown in Figure S1. Clearly, the NiO particle and the TiO₂ layer were observed, whereas the Al₂O₃ layer was hard to assume. Similar situation was also mentioned by other researchers, like a NiO-Al₂O₃ system published by Wu's group². So in this paper, the Al₂O₃ was deposited onto a polished silicon wafer. And the averaged Growth Per Cycle (GPC) value 0.8 Å /cycle was used to evaluate the thickness of Al₂O₃ expected.

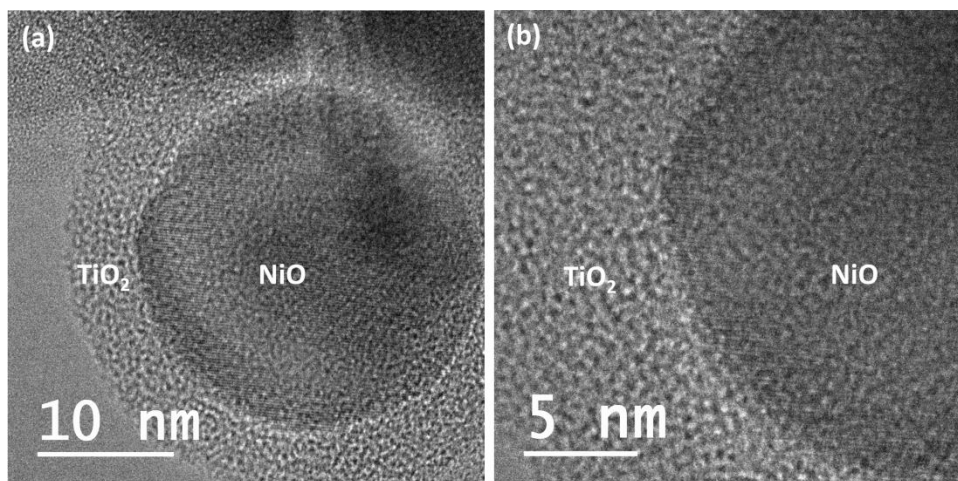


Figure S1. The amplified TEM images of NiO-PB6-Al₂O₃-TiO₂ electrode.

Solar cell characterization

Photocurrent-Voltage (J-V) was measured under AM 1.5 G with light intensity of 100 mW/cm² by a solar simulator (Newport, model 91160).

The Incident-photon to current efficiency (IPCE) was measured by home-made system with a Xenon light source (Spectral Products ASB-XE-175), a monochromator (Spectral Products CM110) and a Keithley multimeter.

Charge lifetime, charge transport time and charge extraction measurements were performed in a Dyenamo tool-box DN-AE01 system. A small square-wave modulation was utilized based on a LED light source (Luxeon Star 1W) and the corresponding transient voltage and current were recorded by a 16-bit resolution data acquisition board (DAQ National Instruments) under open voltage or short circuit condition, respectively. Charge lifetime and charge transport time information was extracted by monoexponential fitting to the corresponding voltage/current response. As for the charge extraction measurements, the solar cells were firstly illuminated for 5 s under open-voltage condition, and then LED light was switched off. Meanwhile, the current-time relationship under short-circuit condition was recorded, and the extracted charges can be integrated accordingly.

Experiment results

Table S1 solar cell performance

	V_{oc} (V)	J_{sc} (μ A)	FF	Eff./%
NiO-PB6-TiO ₂	0.42 \pm 0.05	12.0 \pm 1.6	0.47 \pm 0.07	0.002 \pm 0.0004
NiO-PB6-Al ₂ O ₃ -TiO ₂	0.48 \pm 0.009	22.4 \pm 2.5	0.55 \pm 0.09	0.006 \pm 0.0008
NiO-PB6-Al ₂ O ₃ -TiO ₂	0.48	20	0.66 (best FF)	0.006

Note: the solar cell performance of NiO-PB6-Al₂O₃-TiO₂ with best FF was listed in the bottom line.

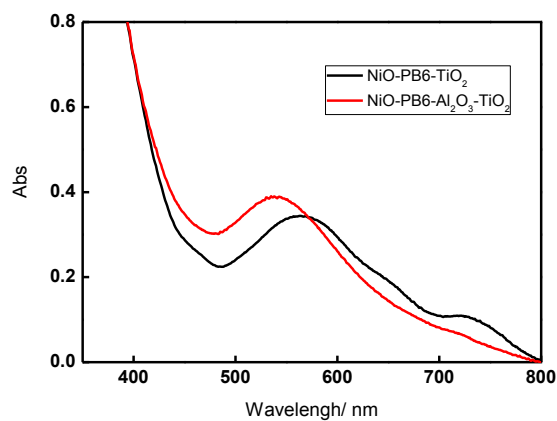


Figure S2. The steady state Uv-vis absorption of NiO-PB6-TiO₂ (black line) and NiO-PB6-Al₂O₃-TiO₂ (red line).

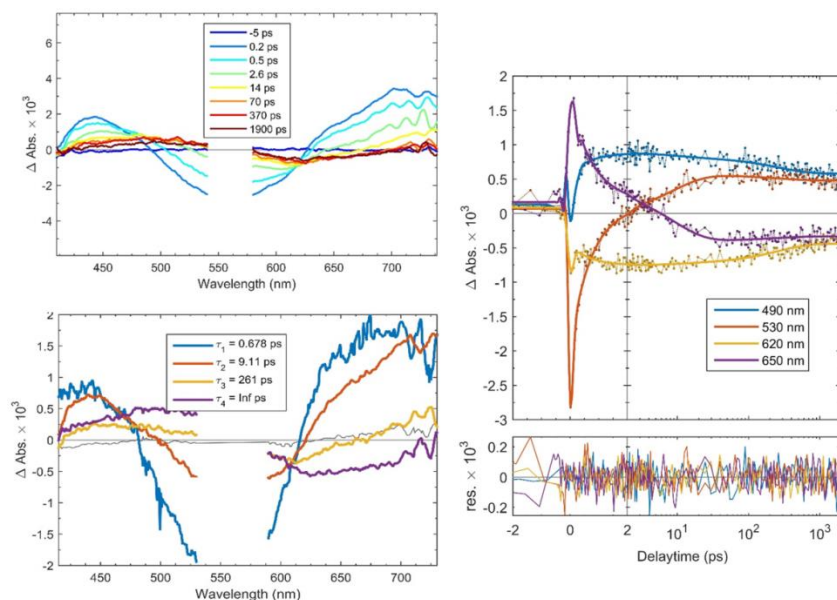


Figure S3. fs transient absorption spectra of NiO-PB6-Al₂O₃-TiO₂ after 560 nm excitation. left: Spectra at different time delays (upper) and decay associated spectra (down): the wavelength dependent amplitude of the components of the triple-exponential fit and an offset, right: fit of the traces at several wavelengths (upper) and residuals (lower).

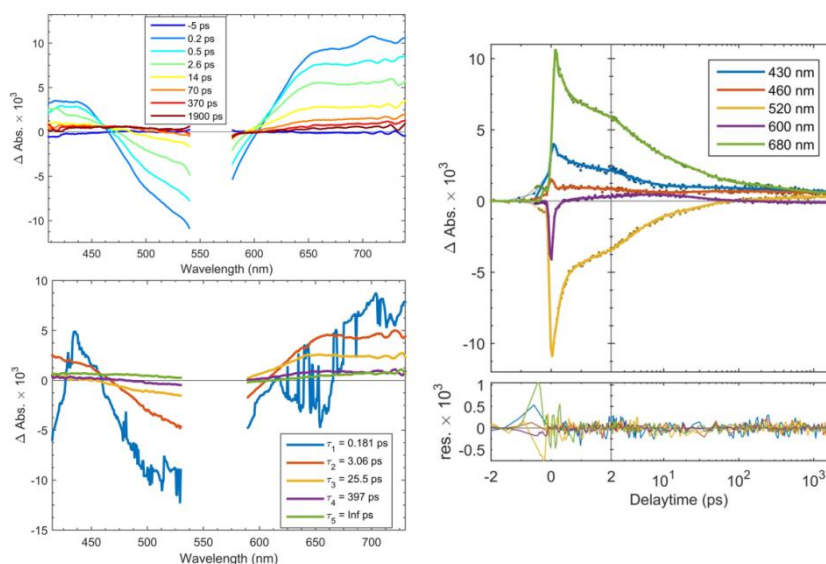


Figure S4. fs transient absorption spectra of NiO-PB6-Al₂O₃ after 560 nm excitation. left: Spectra at different time delays (upper) and decay associated spectra (lower): the wavelength dependent amplitude of the components of the quadruple-exponential fit and an offset, right: fit of the traces at several wavelengths (upper) and residuals (lower).

The transient absorption data for NiO-PB6-Al₂O₃-TiO₂ (Figure S1) is very similar to that of NiO-PB6-TiO₂ published before.¹ The initial shoulder around 640 nm, seen also for NiO-PB6-Al₂O₃ (Figure S2), was assigned to the PB6⁻ anion formed by ultrafast ($t < 120$ fs) hole injection into NiO. The ground state of the dye in NiO-PB6-Al₂O₃-TiO₂ is regenerated with $t_{1/2} \approx 500$ fs. This results in the Stark-shifted ground state spectrum that remains until the end of the optical delay (1.9 ns). After ca. 10 ps (cf. yellow spectrum at 14 ps) there is hardly any further spectral change, meaning that dye regeneration is essentially completed. In the decay associated spectra from the multi-exponential fit, we also see that most of the dye regeneration is described by the first two components τ_1 and τ_2 . The Stark-shift of the ground state PB6 spectrum is due to the electric field created by the charges that are injected into the NiO and TiO₂, respectively. It affects the absorption of the dye molecules, as demonstrated for other dye-semiconductor systems³⁻⁵. Because the lowest excitation has much charge transfer character, the PB6 dye is rather sensitive to the electric field effect.

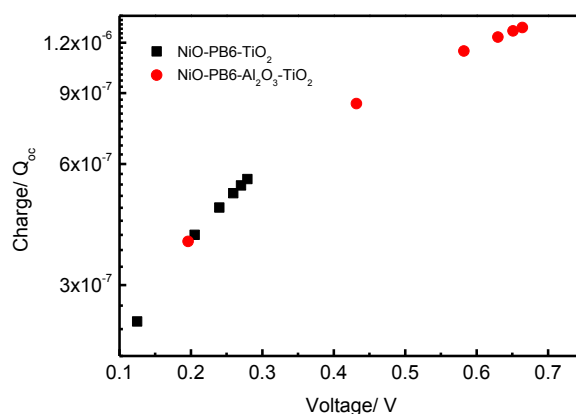


Figure S5. Charge extraction versus voltage measurements under open-voltage condition, NiO-PB6-TiO₂ solar cell (black squared dots), NiO-PB6-Al₂O₃-TiO₂ solar cell (red round dots).

The dye loading experiment: the amount of absorbed PB6 was estimated from a so-called dye desorption experiment^{6,7}. The experiment procedures were described as follow. Firstly, 10 mM phenylphosphonic acid (sigma, 98%) in methanol solvent was prepared. Secondly, the PB6 sensitized NiO sample (1.0 cm*0.9 cm) was dipped into V=2 mL 10 mM phenylphosphonic acid solution for overnight. Then, the absorption coefficient ϵ_{PB6} ($\epsilon_{PB6}=3.04*10^4 M^{-1}cm^{-1}$ in 530 nm) of PB6 in methanol was measured. Eventually, the absorption A_{re} of the replaced PB6 by phenylphosphonic acid was measured. And the absorption of the NiO film before sensitization and after desorption was monitored afterwards.

According to Figure S6a, the absorption of the NiO film before sensitization and after desorption were basically identical, indicating the PB6 dye was fully replaced by the phenylphosphonic acid. No absorption of phenylphosphonic acid in methanol around 530 nm range was observed, shown in Figure S6b. It means the absorption (A_{re}) at 530 nm from the desorption solution was totally from the PB6 dye. So the concentration of the PB6 can be calculated based on Beer-Lambert Law.

$$c_{PB6} = \frac{A_{re}}{L\epsilon_{PB6}} = \frac{0.433}{1.0cm \times 3.04 \times 10^4 M^{-1} / cm^{-1}} = 1.42 \times 10^{-5} M ;$$

$$M_{loading} = \frac{c_{PB6} \times V}{S} = \frac{1.42 \times 10^{-5} mol / L \times 2 \times 10^{-3} L}{0.9cm^2} = 31.6 nmol / cm^2 .$$

c_{PB6} is the concentration of PB6 in the desorption solution; $M_{loading}$ is the PB6 loading amount in the NiO film. S is the geometrical surface area of NiO film utilized in the dye desorption experiment.

So the PB6 loading amount is the NiO used in this paper was ca. 31.6 nmol/cm².

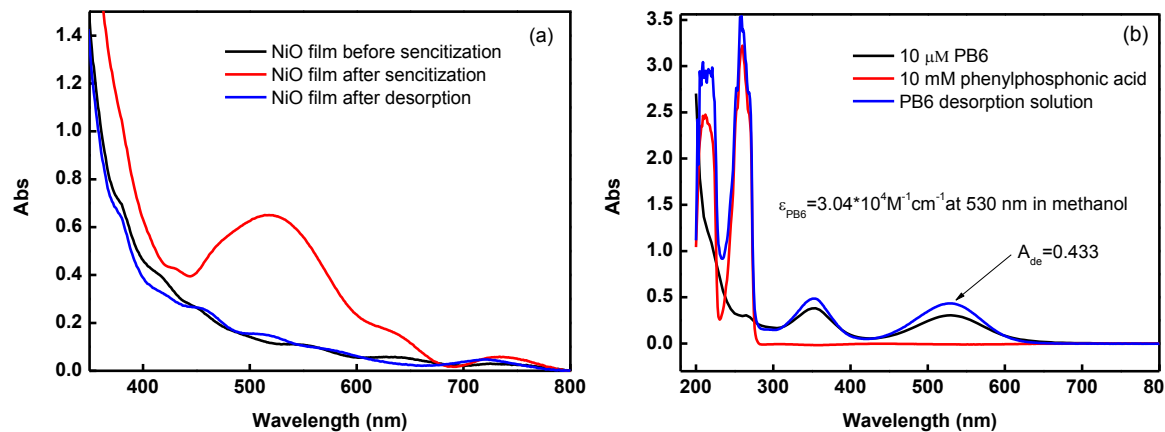


Figure S6 (a) Uv-vis absorption of NiO film before/after sensitization, and the NiO film after dye desorption experiment; (b) Uv-vis absorption of 10 μM PB6 in methanol solvent, 10 mM phenylphosphonic acid in methanol and the desorption PB6 in the phenylphosphonic acid solution.

Reference

- 1 Tian, L.; Föhlinger, J.; Pati, P. B.; Zhang, Z.; Lin, J.; Yang, W.; Johansson, M.; Kubart, T.; Sun, J.; Boschloo, G.; Hammarström, L.; Tian, H., *Phys. Chem. Chem. Phys.* 2018, **20**,36.
- 2 Natu, G.; Huang, Z.; Ji, Z.; Wu, Y., *Langmuir* 2011, **28**,950.
- 3 Ardo, S.; Sun, Y.; Staniszewski, A.; Castellano, F. N.; Meyer, G. J., *J. Am. Chem. Soc.* 2010, **132**,6696.
- 4 Cappel, U. B.; Feldt, S. M.; Schöneboom, J.; Hagfeldt, A.; Boschloo, G., *J. Am. Chem. Soc.* 2010, **132**,9096.

5 Cappel, U. B.; Smeigh, A. L.; Plogmaker, S.; Johansson, E. M.; Rensmo, H. k.; Hammarström, L.; Hagfeldt, A.; Boschloo, G., *J. Phys. Chem. C* 2011, **115**,4345.

6 Ameline, D.; Diring, S.; Farre, Y.; Pellegrin, Y.; Naponiello, G.; Blart, E.; Charrier, B.; Dini, D.; Jacquemin, D.; Odobel, F., *RSC Advances* 2015, **5**,85530.

7 Bergkvist K., "*Dye-sensitized nickel oxide photocathodes for hydrogen evolution from water*"
Master Thesis, 2018, Uppsala University.